

Structural and Raman properties of the tetragonal tungsten bronze ferroelectric $\text{Pb}_{x-3y/2}\text{Gd}_y\text{Ba}_{1-x}\text{Nb}_2\text{O}_6$

L. Zerhouni, Y. Guaaybess, A. Laaraj, E. Elmoussafir, R. Adhiri, M. Moussetad

LIMAT, Faculty of sciences Ben M'sik, Casablanca, Morocco

Copyright © 2016 ISSR Journals. This is an open access article distributed under the **Creative Commons Attribution License**, which permits unrestricted use, distribution, and reproduction in any medium, provided the original work is properly cited.

ABSTRACT: In this work, lead barium niobate tetragonal tungsten bronze structured ceramics modified with Gd^{3+} with the stoichiometric formula $\text{Pb}_{x-3y/2}\text{Gd}_y\text{Ba}_{1-x}\text{Nb}_2\text{O}_6$, where $y=0 - 10$ mol% Gd^{3+} , were fabricate through the solid state reaction method and investigated for structural and Raman properties. The dried powders were calcined at 800°C for 6h and one sample was calcined at 1050°C for 20h. As it can be observed, there is a mixture of tetragonal and orthorhombic phases. The analysis of the Raman spectra allowed a clear identification of the phase evolution Kinetics as a function of the calcining temperature.

KEYWORDS: TTB, ceramics, DRX, Raman spectroscopy.

1 INTRODUCTION

Tetragonal tungsten bronze (TTB) oxides are one of the most important classes of ferroelectrics next to perovskites since the discovery on 1949 of the first material $\text{K}_{0.5}\text{WO}_3$ belonging to this type structure by Magnéli [1]. The literature survey on niobates tungsten bronze type of ferroelectrics showed that a numerous studies have been carried out in binary, ternary and quaternary systems [2–14]. Their structure can be described as a network of slightly distorted oxygen octahedral NbO_6 linked by their corners in such a manner as to form three different types of tunnel (with pentagonal, square and triangular sections) parallel to c -axis [15]. This ferroelectric ceramic are an important class of ferroelectric materials from the viewpoint of basic research an different practical (optical, pyroelectric and piezoelectric) applications, such as multi-layer capacitors, transducers, actuators, ferroelectric random access memory and display, microwave dielectric resonators, filters, phase shifters and pyroelectric detector. These remarkable properties have greatly influenced the researchers to design new and suitable ferroelectric materials. Because of their favorable electro-optic, photo refractive index, elasto-optic, pyroelectric [16], accousto-optic [17] and non-linear optic [18], etc. ferroelectric tungsten bronze niobate materials are classified into three types by the occupation of metal ions:

- (i) Completely filled tungsten bronze (e.g. kLN),
- (ii) Filled tungsten bronze (e.g. PBN, SBN).

The ceramics of the lead barium niobate $\text{Pb}_x\text{Ba}_{1-x}\text{Nb}_2\text{O}_6$ series had been studied in early years. It was shown in phase diagram that the solid solution of $x\text{PbNb}_2\text{O}_6(1-x)\text{BaNb}_2\text{O}_6$ has an orthorhombic structure for $0.63 < x < 1$, a tetragonal two-phase mixed structure for $0.53 < x < 0.63$. The structure of lead barium niobate (PBN) is an incompletely filled TB-type structure as in SBN crystals.

In this work, we report the growth, structural and Raman scattering characterization of the new family of ferroelectric compounds of TTB type $\text{Pb}_{x-3y/2}\text{Gd}_y\text{Ba}_{1-x}\text{Nb}_2\text{O}_6$ (PGBN) as a function of y ($0 \leq y \leq 10$).

2 SAMPLE PREPARATION AND EXPERIMENTAL DETAILS

Analytical reagent grade powders of lead oxide (purity 98%) (PbO), barium oxide (BaO, purity 95%), niobium pentoxide (Nb_2O_5 , purity 99.99%) and gadolinium oxide (Gd_2O_3 , purity 99.99%) were used as starting materials to yield stoichiometric compositions (Tab.1) and prepared through the solid state reaction method. The raw materials were weighed according to their stoichiometric ratios to form $\text{Pb}_{0.55-3y/2}\text{Gd}_y\text{Ba}_{0.45}\text{Nb}_2\text{O}_6$. An excess 3wt% PbO added compositions had shown consistency in phase formation since the starting stoichiometric materials participate in the chemical reaction to form end product, and excess PbO compensates the lead volatilization during high temperature sintering. The butch powders were milled using in agate mortar. The dried powders were calcined at 800°C for 6h, except one sample was dried at 650°C for 6h and calcined at 1050°C for 20h in crucible by maintaining air pressure.

Table 1. Gd^{3+} modified tetragonal tungsten bronze structured PBGN ceramics

y(mol%)	Formula of PBGN	Sample abbreviation
0	$\text{Pb}_{0.55}\text{Ba}_{0.45}\text{Nb}_2\text{O}_6$	PBGN-0
2	$\text{Pb}_{0.52}\text{Gd}_{0.02}\text{Ba}_{0.45}\text{Nb}_2\text{O}_6$	PBGN-2
8	$\text{Pb}_{0.43}\text{Gd}_{0.08}\text{Ba}_{0.45}\text{Nb}_2\text{O}_6$	PBGN-8
10	$\text{Pb}_{0.40}\text{Gd}_{0.1}\text{Ba}_{0.45}\text{Nb}_2\text{O}_6$	PBGN-10

3 RESULTS AND DISCUSSIONS

3.1 CHEMICAL BAND ANALYSIS

The infrared spectral analysis is effectively used to understand the chemical banding and it provides information about molecular structure of the synthesized compound. The IR-spectrum is shown in figure1. In the IR-spectrum, intense absorption is observed in the range 900 - 500 cm^{-1} . The sharp absorption positioned around 670 cm^{-1} and 819 cm^{-1} were assigned to Nb-O stretching. The band centered at 878 cm^{-1} was assigned to Nb-O stretching of the niobium band with apical oxygen in the $[\text{NbO}_6]$ octahedron.

The sharp absorption peak at 3470 cm^{-1} indicating the presence of hydroxide group (OH-) result from surface absorbed atmosphere (like moisture and humidity)[19]. Peaks around 1646 cm^{-1} and 1755 cm^{-1} may be attributed to O-H bending vibration. The bands at 816 cm^{-1} was associated with coupling mode between Nb-O stretching modes of barium niobate (BaNb_2O_6) [20]. The band at 880 cm^{-1} can be assigned to the Nb-O stretching of the niobium band with apical oxygen in the $[\text{NbO}_6]$ octahedron of $\text{NaSr}_2\text{Nb}_5\text{O}_{15}$ nanostructured powder [21].

The number of bands derived in the wavenumber range from 600 to 900 cm^{-1} suggests that the vibrations are due to the Nb-O bands observed in the infrared spectrum of the $\text{Pb}_{0.52}\text{Gd}_{0.02}\text{Ba}_{0.45}\text{Nb}_2\text{O}_6$ powder (Fig.2).the band positions and band characteristics are assigned as listed in Table.2.

Table 2. Assignment of the FT-IR absorption bands

Assignments	Wavenumber (cm^{-1})	Intensity	Ref
Stretching of the Nb-O bonds ^a	670	strong	[20]
Stretching of the Nb-O bonds ^a	819	low	[20]
Stretching of the Nb-O bonds ^b	878	medium	[21]

a slightly distorted NbO_6 octahedra

b Distorted NbO_6 octahedra

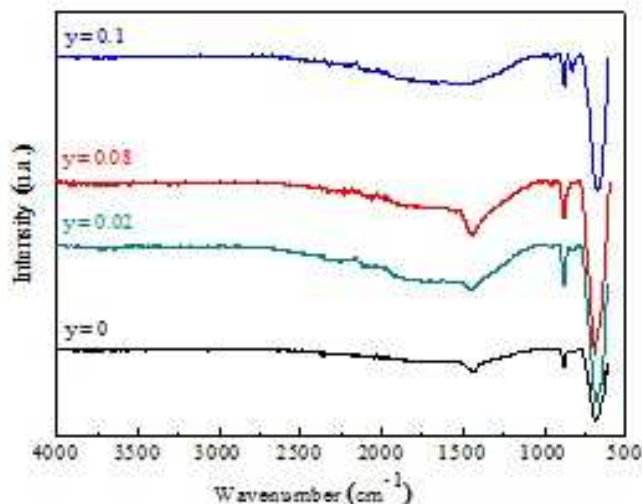


Fig.1: IR spectra from $\text{Pb}_{(0.55-3y/2)}\text{Gd}_y\text{Ba}_{0.45}\text{Nb}_2\text{O}_6$ ($0 \leq y \leq 0.1$) ceramics calcined at 800°C for 6h

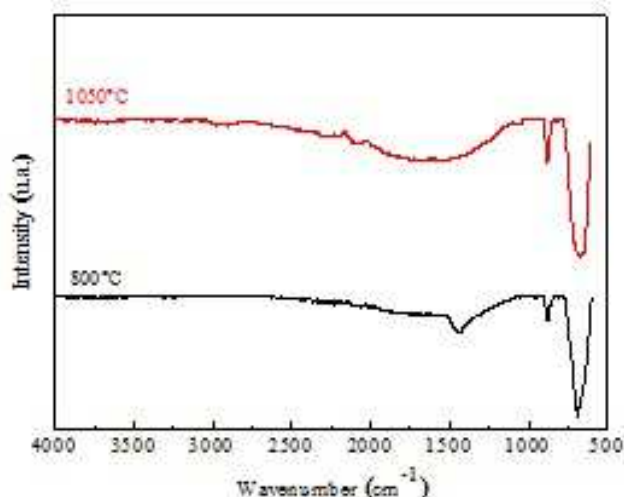


Fig.2: IR spectra from $\text{Pb}_{0.52}\text{Gd}_{0.02}\text{Ba}_{0.45}\text{Nb}_2\text{O}_6$ ceramics calcined at 800°C for 6h and 1050°C for 20h

3.2 STRUCTURAL CHARACTERIZATIONS

X-ray measurements were performed using a analytical X'pert Pro MPD diffractometer with a copper radiations $\lambda\alpha=1.54 \text{ \AA}$. Working in transmission (Debye-Scherrer) mode, this diffractometer is provided with a cylindrical furnace which permits us to collect X-ray diagrams versus temperatures. The sample powders were sealed in a glass capillary and the transmitted beam is focused to a Rapid linear solid state (X'Celerator) detector.

Fig.3 shows the room temperature XRD patterns of PGBN ($\text{Pb}_{0.55-3y/2}\text{Ba}_{0.45}\text{Nb}_2\text{O}_6$) with ($y=0, 0.2, 0.08$ and 0.1) powders calcined at 800°C and Fig.2 exhibits XRD patterns of PGBN-2 calcined at 800°C and 1050°C . The patterns of all compositions of the powders are crystallizing in a TB-type structure without secondary phases being present within the detection limits of our instrument. It is noting that the intensity of some peaks is weak. Peaks around 28.7° and 29.4° for all samples calcined at 800°C . Which correspond to the characteristic reflection (221) and (400) indicate appearance of tetragonal phase, with two main diffraction peaks of (151) and (350) are assigned to orthorhombic phase. From the figure, it is clear that the X-ray diagram of PGBN compounds are quite similar except few reflection peaks which are not observed in PGBN-10 happening at 2θ of 44.1° . This means that all powders are shown to be a mixture of tetragonal and orthorhombic phase structure.

Furthermore, fig.4 exhibits the XRD patterns of $Pb_{0.52}Gd_{0.02}Ba_{0.45}Nb_2O_6$ ceramics calcined at $800^\circ C$ for 6h and $1050^\circ C$ for 20h. All peaks show composition shifts, similar to that mentioned in the discussion of Fig.3. The presence of PGBN-2 annealed at $1050^\circ C$, two diffraction peaks at 27.6° and 32° . As it can be observed, there is a mixture of tetragonal and orthorhombic phases, as it was confirmed to be in Raman. The increasing the temperature improves the crystallization powders. The cell parameters were evaluated by the minimum square roots method. The tetragonal phase presented the following values: $a=b= 12.3401 \text{ \AA}$ and $c= 4.004 \text{ \AA}$. The values obtained for the orthorhombic phase were: $a=17.5140\text{\AA}$, $b=17.637\text{\AA}$ and $c= 7.1382 \text{ \AA}$. finally, in analogy with PBN63/37 powder calcined at $1200^\circ C/4h$ [32].

For PGBN powder calcined at $800^\circ C$ the lattice constants a , b and c were calculated and were presented in Table.3. The volume of elementary cell decrease with increasing y . These results lattice parameters of PGBN may be to the ionic radius of $Gd^{3+}(r=1.02 \text{ \AA})$ is smaller than those of $Ba^{2+}(r=1.35\text{\AA})$ and $Pb^{2+}(r=1.20\text{\AA})$.

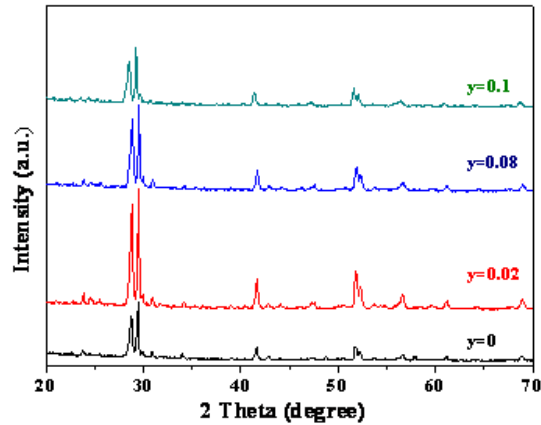


Fig.3: The XRD patterns of $Pb_{(0.55-3y/2)}Gd_yBa_{0.45}Nb_2O_6$ ($0 \leq y \leq 0.1$) ceramics calcined at $800^\circ C$ for 6h

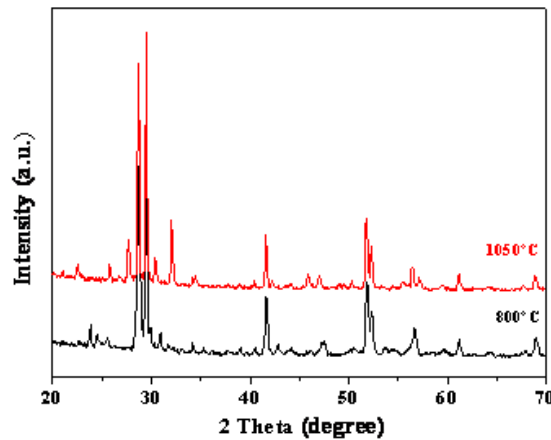


Fig.4: The XRD patterns of $Pb_{0.52}Gd_{0.02}Ba_{0.45}Nb_2O_6$ ceramics calcined at $800^\circ C$ for 6h and $1050^\circ C$ for 20h

3.3 RAMAN SPECTROSCOPY

The x-ray diffraction study revealed that the as-prepared powder PGBN is a mixture of tetragonal and orthorhombic. To investigate more on the structural details of PGBN-2, Raman spectra of the sample are also recorded and shown in Fig.5.

the Raman spectra of sample with $y=0.02$, calcined at $800^\circ C$, the emerging of lines at $87.8, 137.4, 172, 196.8, 240.8, 315.8, 355.2, 470, 671 \text{ cm}^{-1}$ can be seen, which could be a characteristic feature of a PGBN-2 tungsten-bronze phase. Corresponding to the symmetry species, One weak B1 phonon at 172 cm^{-1} and there are 137 cm^{-1} optical phonon modes in the unit cell, it is possible that several nearly degenerate modes may occur and appear as one band [30].

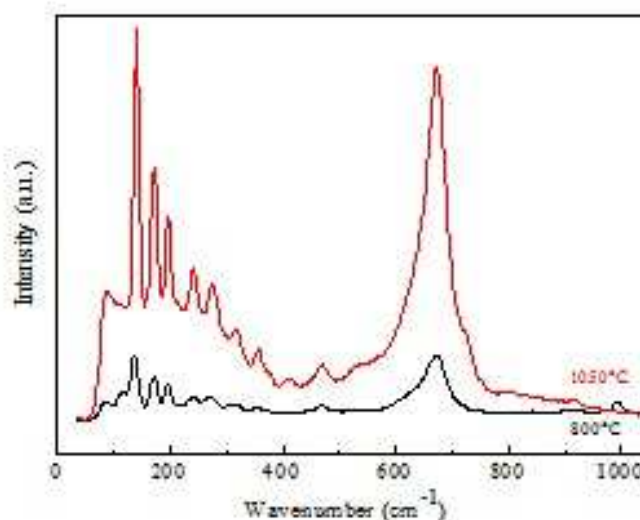
Table.3: Lattice parameter, volume for $\text{Pb}_{0.55-3y/2}\text{Ba}_{0.45}\text{Nb}_2\text{O}_6$ compounds

Sample	Lattice parameter			Volume(\AA^3)	Lattice parameter			Volume(\AA^3)
	Tetragonal phase				orthorhombic phase			
	a(\AA)	b(\AA)	c(\AA)		a(\AA)	b(\AA)	c(\AA)	
PGBN-0	12.6736	12.6736	4.0068	643.6015	17.4068	17.5136	7.3302	2234.6928
PGBN-2	12.3133	12.3133	4.0946	620.8268	17.6767	17.8063	6.7776	2133.3369
PGBN-8	12.3177	12.3177	4.0892	620.4575	17.5316	17.9034	6.6213	2078.2989
PGBN-10	12.3176	12.3176	4.0890	620.3964	17.2285	17.3226	6.3980	1909.4495

The very weak peak at 355 cm^{-1} is the A_1 mode of Nb-O elongation [31]. The two modes 240 cm^{-1} and 670 cm^{-1} are well resolved when y increases, but their frequencies do not change much with y ($y=0-10\text{ mol}\% \text{ Gd}^{3+}$). This is similar to the 248 and 628 cm^{-1} mode observed in LiNbO_3 and to the 242 cm^{-1} and $618-665\text{ cm}^{-1}$ modes reported for $\text{Pb}_{2(1-x)}\text{K}_{1+x}\text{Gd}_x\text{Nb}_5\text{O}_{15}$ [15]. finally, in analogy with perovskites [22]. At the calcining temperature of 1050°C , the vanishing of the peak at about 1000 cm^{-1} which attributed to the terminal Nb-O stretching vibration is observed as a sharp highly intense peak in Fig.5 [23-24]. The spectra are similar and show two strong peak around 275.8 cm^{-1} and 672 cm^{-1} . Comparing the obtained spectra with the Raman for the majority of TTB ferroelectric materials [25-27], it is easy to determine the first characteristic Raman peaks of the internal modes of NbO_6 in PGBN to be 240 cm^{-1} (O-Nb O bending), with the second classified as Nb-O stretching vibration that show intense peaks at 671 cm^{-1} . These two peaks mostly involve the transverse A_1 symmetry. While the Raman spectra display some differences, mainly in the low frequency region, in particular, there are two additional peaks at about 116.6 cm^{-1} and 137.4 cm^{-1} emerging from the broad band in the low frequency region.

Such different behavior of O-Nb-O bending and Nb-O stretching vibration can be attributed to the large number of modes involved in the spectral range between 172 cm^{-1} and 318 cm^{-1} as reported in the literature on TTB ferroelectric material [25-26]. The lowest frequency band 87 cm^{-1} of appreciable intensity is due to the lattice vibrations.

The Raman spectrum show less well defined peaks, agreeing with the fact that these materials are not single phased, but composed by a mixing of orthorhombic and other tungsten- bronze phases, as also observed in the sequence reaction of strontium barium niobates [28]. For composition $\text{Pb}_{0.52}\text{Gd}_{0.02}\text{Ba}_{0.45}\text{Nb}_2\text{O}_6$, intermediary phase started to develop between 600°C and 800°C , the continuous reaction of Nb_2O_5 into these phase is clear. Calcined powders at 1050°C of these compositions presented mainly, at room temperature, a mixture of two TB phases : the orthorhombic and tetragonal. This feature is compatible with $\text{Pb}_{0.56}\text{Ba}_{0.44}\text{Nb}_2\text{O}_6$ and $\text{Pb}_{0.6}\text{Ba}_{0.4}\text{Nb}_2\text{O}_6$ treated at 1100°C , suggesting the reaction to form intermediate phase was not single phased [29]. Finally, the Raman results indicated that for these samples completely reacted $\text{Pb}_{0.52}\text{Gd}_{0.02}\text{Ba}_{0.45}\text{Nb}_2\text{O}_6$ structure was reached at temperatures lower than 1240°C . The increase in the Pb/Gd content to a lowering of the orthorhombic phase formation with increase of the tetragonal phase formation. The Pb/Gd ratio plays an important part in achievement of calcining temperature and reduce of the disorder in the TTB structure when going from orthorhombic to the tetragonal phase [29-15].

Fig.5: Raman spectra from $\text{Pb}_{0.52}\text{Gd}_{0.02}\text{Ba}_{0.45}\text{Nb}_2\text{O}_6$ calcined at 800°C for 6h and 1050°C for 20h

4 CONCLUSION

We prepared a series of new family of TTB ferroelectric materials $\text{Pb}_{x-3y/2}\text{Gd}_y\text{Ba}_{1-x}\text{Nb}_2\text{O}_6$ with $0 \leq y \leq 1$ using a solid reaction technique by coupled (Ba-Pb) and (Gd-Pb) substitutions. X-ray diffraction indicates that the powders are pure and crystallize in a TTB-type structure.

The analysis of the Raman, IR and XRD spectra allowed a clear identification of the phase evolution kinetics as a function of the calcining temperature. The results showed the occurrence of the orthorhombic and tetragonal phases for all compositions at the final PGBN structure. From the XRD results, it was clear that the solid solution was reached at a temperature above 800°C and elsewhere, the XRD spectra showed at 1050°C the total formation was completed, a lower temperature than those reported by the literature [32]. An enhancement of physical properties can be expected near these concentrations of Gd. It would be interesting therefore to study these compounds more carefully around $x \sim 0.25$ with tightened steps of y .

This work anticipates our future investigation of the ferroelectric TTB family that will allow us to compare the properties of ceramic compound with single-crystal result and to study the dielectric desorption by impedance spectroscopy.

ACKNOWLEDGEMENTS

The authors gratefully acknowledge S.Sayouri professor of faculty of sciences Fès for his scientific support of this work.

REFERENCES

- [1] A. Magnéli, *Arkiv Kemi* 1 (1949) 213.
- [2] M. Josse, O. Bidault, F. Roulland, E. Castel, A. Simon, D. Michau, R. Von der Mühl, O. Nguyen, M. Maglione, *Solid State Sci.* 11 (2009) 1118.
- [3] Annie Simon, Jean Ravez, *Comptes Rendus Chim.* 9 (2006) 1268.
- [4] J. Ravez, B. Elouadi, *Mater. Res. Bull.* 10 (1975) 1249.
- [5] K. Sambasiva Rao, P. Murali Krishna, T. Swarna Latha, D. Madhava Prasad, *Materials Science and Engineering B.* 131 (2006) 127–134.
- [6] Fang Liang, Zhang Hui, Wu Bolin, Yuan Runzhang, *Progress in Crystal Growth and Characterization of Materials.* 40 (2000) 161–165
- [7] N.S. VanDamme, A.E. Sutherland, K. Bridger, S.R. Winzer, L. Jones, *J. Am. Ceram. Soc.* 74 (1991) 1785.
- [8] L.E. Cross, *Ferroelectrics* 151 (1994) 305.
- [9] M. Dong, J.M. Reau, J. Ravez, *Solid State Ionics* 91 (1996) 183.
- [10] P.V. Bijumon, V. Kohli, O. Prakash, M.R. Verma, M.T. Sebastian, *Mater. Sci. Eng. B* 113 (2004) 13.
- [11] S.R. Shannigrahi, R.N.P. Choudhary, A. Kumar, H.N. Acharya, *J. Phys. Chem. Solids* 59 (1998) 737.
- [12] R. Palai, R.N.P. Choudhary, H.S. Tewari, *J. Phys. Chem. Solids* 62 (2001) 695.
- [13] P. Prabhakar Rao, S. K. Ghosh, Peter Koshy, *Journal of Materials Science: Materials in Electronics.* 12 (2001) 729-732.
- [14] Emma E. McCabe, Anthony R. West, *J. Solid State Chem.* 183 (2010) 624.
- [15] Y. Amira, Y. Gagou, A. Menny, D. Mezzane, A. Zegzouti, M. Elaammani, M. El Marssi, *Solid State Commun.* 150 (2010) 419.
- [16] A.M. Glass, *J. Appl. Phys.* 40 (1969) 4699.
- [17] E.L. Venturini, E.G. Spencer, A.A. Ballman, *J. Appl. Phys.* 40 (1969) 1622.
- [18] S.C. Abrahams, P.B. Jamieson, J.L. Bernstein, *J. Chem. Phys.* 54 (1971) 2355.
- [19] S.N. Matthad, R.N. Jadhav, R.P.P.V. Puni. *Science of Advanced Materials* 4, no. 12, pp. 1276–1281, 2012.
- [20] S. N. Mathad, Vijaya Puri. *International Scholarly Research Notices* (2014) 1-6
- [21] S. Lanfredi, D. Genova, L. Brito, A. Lima, M. Nobre. *J. Solid Stat Chem.* 189(2011) 990-1000
- [22] B. Manoun, S. Benmokhtar, L. Bih, M. Azrou, Aezzahi, A. Ider, M. Azdouz, H. Annersten, P. Lazor, *J. Alloys Compd.* 509(2010)66.
- [23] E. Husson, Y. Repelin, N.Q. Dao, H. Brusset. *J. Phys. chem.* 66(1977)5173-5180
- [24] F.D. Hardcastle and I.E. Solide. *state ionics.* 45(1991)201-203
- [25] G. Burns, J.D. Axes. *D.F.O'Kan solide state. commin.* 7(1969)933
- [26] K.N. Sungh, P.K. Bajpai. *International. Academy of Physical Sciences.* 14 (2010) 501-510
- [27] R.F. Schaufele. M.J. Weber. *PHYS. Rev.*152(1966)705
- [28] T.T. Fang. N.T. Wu, F.S. Shiau, *J. Mat. Sci. Letters* 13(1994)1746-1747

- [29] F. Lanciotti Jr, P. S. Piizani, I.A. Santos, C.V. do Carmo, D. Garcia, J.A. Eiras. J. Phys. Chemistry of solides. 62(2001) 1247-1250
- [30] Melanie M. T. Ho, C. L. Mak, K. H. Wong Journal of the European Ceramic Society 19 (1999) 1115-1118
- [31] A. Belboukhari, D. Mezzane Y. Gagou, M. Elmarssi, I. Luk'yanchuk, A. Zegzouti, P. Saint-Grégoire. M.J. Condensed Matter Society. 12(2010)103-107
- [32] V.L. Arantes R.N. De Paula. I.A. Santos, D.Garcia. J.A. eiras journal of matériels science letters. 19(2000)1677-1679.